

Nanoscale photon management in silicon solar cells

Sangmoo Jeong, Shuang Wang, and Yi Cui

Citation: *J. Vac. Sci. Technol. A* **30**, 060801 (2012); doi: 10.1116/1.4759260

View online: <http://dx.doi.org/10.1116/1.4759260>

View Table of Contents: <http://avspublications.org/resource/1/JVTAD6/v30/i6>

Published by the AVS: Science & Technology of Materials, Interfaces, and Processing

Related Articles

Status and prospects of Al₂O₃-based surface passivation schemes for silicon solar cells
J. Vac. Sci. Technol. A **30**, 040802 (2012)

Amorphous and nanocrystalline silicon thin film photovoltaic technology on flexible substrates
J. Vac. Sci. Technol. A **30**, 04D108 (2012)

Room temperature atomic layer deposition of Al₂O₃ and replication of butterfly wings for photovoltaic application
J. Vac. Sci. Technol. A **30**, 01A146 (2012)

High-efficiency and highly stable a-Si:H solar cells deposited at high rate (8 Å/s) with disilane grading process
J. Vac. Sci. Technol. A **29**, 061201 (2011)

Photovoltaic manufacturing: Present status, future prospects, and research needs
J. Vac. Sci. Technol. A **29**, 030801 (2011)

Additional information on *J. Vac. Sci. Technol. A*


Journal Homepage: <http://avspublications.org/jvsta>

Journal Information: http://avspublications.org/jvsta/about/about_the_journal

Top downloads: http://avspublications.org/jvsta/top_20_most_downloaded

Information for Authors: http://avspublications.org/jvsta/authors/information_for_contributors

ADVERTISEMENT




Aluminum Valves with Conflat® Flanges

Less Outgassing Than Stainless
Mate to Stainless Steel Conflats
Sizes From 2.75 to 14 inch O.D.
Leak Rate Less Than 10⁻¹⁰ SCC/S

Visit us
at Booth # 300
in Tampa

Prices & Specifications
vacuumresearch.com



Nanoscale photon management in silicon solar cells

Sangmoo Jeong and Shuang Wang

Department of Electrical Engineering, Stanford University, Stanford, California 94305

Yi Cui^{a)}

*Department of Materials Science and Engineering, Stanford University, Stanford, California 94305
and Stanford Institute for Materials and Energy Science, SLAC National Accelerator Laboratory,
2575 Sand Hill Road, Menlo Park, California 94025*

(Received 16 July 2012; accepted 28 September 2012; published 18 October 2012)

Light absorption in a photovoltaic device becomes critical as the thickness of an absorber layer is decreased to reduce cost. To enhance light absorption, photon management at the nanoscale has been studied because conventional methods, which are based on micrometer-sized structure, do not work well for thinner solar cells. This article reviews recent progress in photon management on the nanoscale for increasing light absorption in Si solar cells. The methodology for the absorption enhancement will be discussed, followed by advances in nanofabrication techniques that make the methodology a scalable and viable solution. The authors conclude with a discussion of the challenge of photon management schemes and future directions for light trapping in ultra-thin Si solar cells. © 2012 American Vacuum Society. [<http://dx.doi.org/10.1116/1.4759260>]

I. INTRODUCTION

One of the most critical challenges facing human society is how to fuel the global economy in an era of exceptional growth, while reducing the amount of greenhouse gases, such as carbon dioxide, being emitted. Energy security is another major challenge in its own right: more than 80% of global oil and natural gas reserves are located in a few of countries, but most of them are located far away from the major energy consumers.¹ In contrast, renewable energy resources, such as solar and wind, can be accessed easily in most of the world. In particular, the solar energy delivered to the earth per year, 23 000 terawatt (TW), is three-order magnitude larger than the energy consumed in the world per year, 16 TW, which indicates that photovoltaic systems have the potential to play an essential role in addressing the challenge of climate change, as well as offering important energy security benefits. For power generation, low-cost fossil fuel has, however, been preferred to renewable energy because of the latter's higher cost. In order for a photovoltaic system to be a more attractive energy solution, its cost must be significantly reduced. For instance, the module cost of the silicon (Si) photovoltaic system, of which 80–90% of the current photovoltaic industry consists, needs to be reduced by at least more than 50%, according to the U.S. Department of Energy.²

To make cost-effective photovoltaic systems, thin-film solar cells, which have an absorber layer with a thickness less than 5 μm , have been developed. For example, copper indium gallium selenide (CIGS) solar cells fabricated on cheap soda-lime glass substrates have achieved the power

conversion efficiency of 20.3%.³ This high efficiency at the small size cells is significant: it implies that low-cost thin-film solar cells are able to compete with Si solar cells in terms of power conversion efficiency. Another example is cadmium telluride (CdTe) solar cells, which is a leading technology in decreasing the photovoltaic system cost: they have reduced a manufacturing cost of modules to less than \$1/Watt in 2011 with a cell efficiency above 17% and a module efficiency above 14%. Also, more than a gigawatt scale of the installation of CdTe solar cells has resulted in business success. However, these inorganic thin-film solar cells have limitations: indium (In) and tellurium (Te), which are components of CIGS and CdTe solar cells, are not available in sufficient quantities to support the world's fast-growing energy demand. Other thin-film solar cells have been developed from organic materials. Polymer-based or small molecule-based cells are attractive as low-cost photovoltaic devices because they can be fabricated at low temperatures, less than 200 °C, on cheap and flexible substrates. In particular, the efficiency of polymer-based solar cells has increased from 5% to more than 10% within the last five years.^{4,5} However, significant improvement of efficiency is still needed and the long durability of most organic solar cells is still a question to guarantee stable power conversion efficiency over 20 years,^{6,7} which is a standard warranty period for a photovoltaic system. Niche applications for organic solar cells may emerge, but their segment in the whole photovoltaic industry would not be significant. Due to all of these drawbacks of thin-film photovoltaic technologies, Si solar cells, which have no limitation for use in terms of abundance, toxicity, and stability, will likely continue to be a major player in the industry.

^{a)}Electronic mail: yicui@stanford.edu

The highest power conversion efficiency of a single-crystalline Si solar cell is 25%, which is close to the theoretical limit, 30%.^{8,9} The Si solar cell with the world-record in efficiency has micrometer-sized inverted pyramids on the front surface covered with double-layer antireflection coating.^{10,11} This structure decreases reflection and scatters incoming light into large angles, but the required thickness of the Si is still approximately 300 μm . In order to decrease the Si thickness by 50–95%, there needs to be a smart design to improve the light absorption in a thin Si layer. The conventional surface texturing used for a crystalline Si solar cell is too large to be implemented in thin Si devices. Therefore, various light trapping schemes on the nanoscale have been developed. In addition, effective light trapping can allow us to use material with a higher impurity level, which is less expensive. This lower-quality material has shorter carrier diffusion length, which indicates that the absorber layer should be thin enough to collect photon-generated charge carriers effectively. Light trapping on the nanoscale allows a thin layer of low-quality Si to not only absorb more light but also extract photon-generated charge carriers with minimal loss. Thin Si also effectively concentrates the sunlight for possible efficiency enhancement. This article will review the work of nanoscale photon management in Si solar cells mainly based on our own work. We will include single crystalline, nanocrystalline and amorphous Si.

II. METHODOLOGY

Light absorption in a material can be increased by two mechanisms: antireflection from the surface and light-scattering inside the material. When the material is thick enough to absorb most of the light in a single path, the former effect plays a major role in the enhancement of light absorption. However, for a thin material, both effects must be considered and studied to maximize the enhancement of light absorption.

A. Photon management: antireflection

Reflection of light, R , at an interface of two media is caused by the difference in their refractive index, expressed as

$$R = \left(\frac{n_1 - n_2}{n_1 + n_2} \right)^2, \quad (1)$$

where n_1 and n_2 are the refractive indices of the two media. Standard transparent glass reflects approximately 4% of visible light (400–1200 nm wavelength), which is due to the difference in the refractive index, 1.0 for air and 1.5 for glass. A flat silicon surface without any antireflection layer reflects approximately 40% of light at the 600 nm wavelength. One common method for reducing the reflection is to add an anti-reflection coating layer whose refractive index is between those of the substrate and air. For conventional crystalline Si solar cells, a film of silicon oxide (SiO_2) or silicon nitride (Si_3N_4) is deposited for the antireflection layer.^{12,13} This film reduces the reflection not only by providing the intermediate

value of the refractive index, but also by having a thickness that produces destructive interference of the incoming light. However, the coating layer is effective only within a limited spectrum of light at a certain incident angle. Further reduction of reflection can be achieved by depositing multiple layers with graded refracted indices.^{14,15} In order to have a structure with an ideally graded index profile, the surface texturing on the nanoscale has been studied to find appropriate tapered structures.^{16–21} Figure 1(a) shows the effective refractive index profiles of three different structures of amorphous Si (a-Si:H): planar structure, nanowires, and nanocones. The effective refractive index changes more gradually as the structure changes from the planar one to nanowires, and to the nanocones. Because the gradual change of the refractive index minimizes the reflection [the numerator in Eq. (1) approaches zero], the nanocones can achieve higher light absorption than other structures, as shown in Figs. 1(b) and 1(c). Especially, the absorption data plotted as a function of the incident angle [Fig. 1(c)] demonstrate the importance of the nanostructures for solar cells. A planar solar cell needs to keep facing the Sun for absorbing as much sunlight as possible during the day because the light absorption decreases significantly as the incident angle of light deviates from zero. However, a solar tracking unit can increase the cost of a photovoltaic system; thus, it is normally used only for concentrator applications. This additional cost can be saved by the nanocone structure; when the incident angle of light increases from zero to 60°, the light absorption in the nanocone structure remains over 90%, but that of the planar structure decreases from 80% to 50%. In addition, the superior antireflection effect of the nanocones compared to the conventional double-layer antireflection coating has the potential to decrease the material thickness by more than a factor of 10. As shown in Fig. 1(d), a 50 μm thick Si substrate with 400-nm height nanocone arrays has higher absorption than a 500 μm thick Si substrate coated with a double antireflection layer.²²

B. Photon management: light-scattering

Light scattering inside the absorber material is another method for the improvement of light absorption. The absorption coefficient of a material decreases exponentially as the wavelength of incident light increases: for example, the coefficient of Si is $1.2 \times 10^5 \text{ cm}^{-1}$ at 400 nm wavelength, and $9.5 \times 10^2 \text{ cm}^{-1}$ at 800 nm.²³ In order to absorb most of the incident light in a thin layer, the light needs to be scattered so that its optical path length increases as much as possible inside the material. Si, in particular, has a relatively low absorption coefficient, compared to other semiconductors, such as gallium arsenide (GaAs) or germanium (Ge): for 800 nm wavelength of light, the coefficients of GaAs and Ge are $1.3 \times 10^4 \text{ cm}^{-1}$ and $4.9 \times 10^4 \text{ cm}^{-1}$, respectively.²³ Thus, for a conventional Si solar cell, various textured structures in microscale have been studied for the light scattering.^{24–26} Among these structures, a random textured structure (i.e., a Lambertian structure) is known to be the most effective one: the optical path length can be enhanced

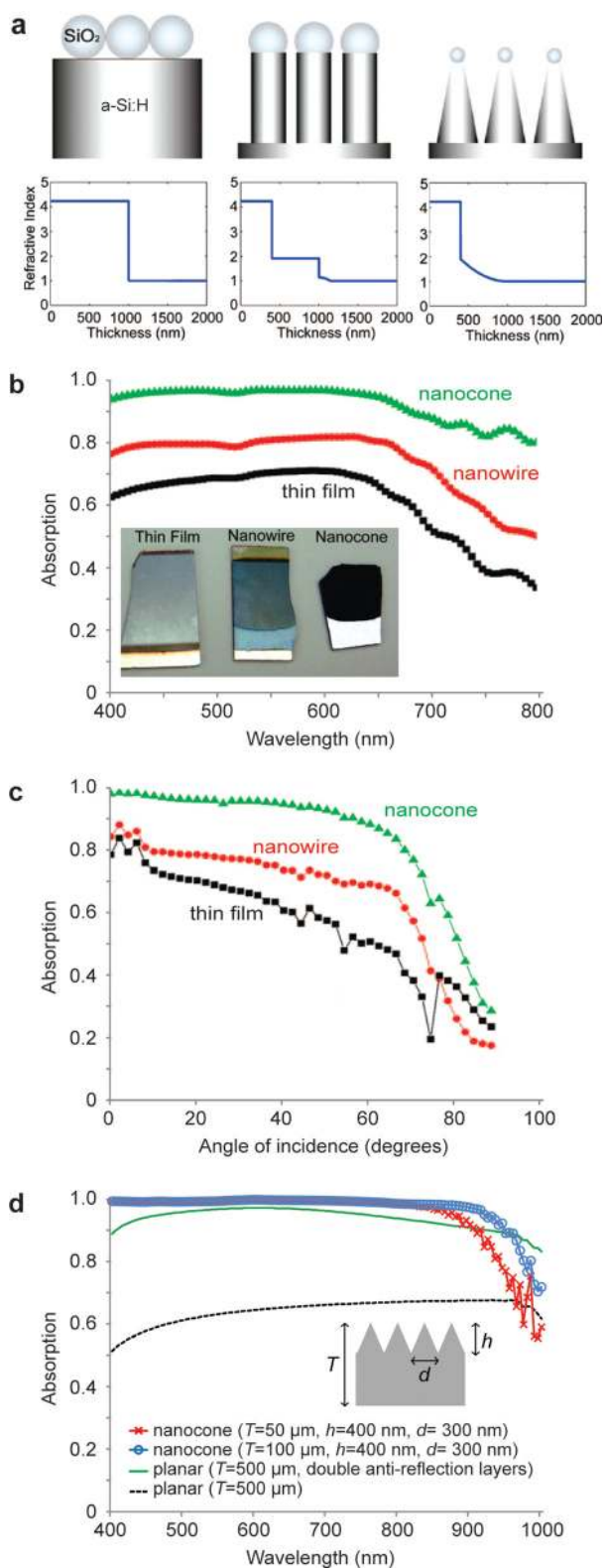


Fig. 1. (Color online) (a) Schematics of nanostructures with effective refractive index profile. (b) and (c) Optical absorption data. Measured absorption data of 1 μm thick amorphous Si with three different structures as a function of (b) wavelength and (c) incident angle. (d) Calculated absorption data of crystalline Si nanocones with different thickness of substrates and crystalline Si planar structures with and without anti-reflection coating layers. Figures reproduced with permission: (a)–(c) from Zhu *et al.*, *Nano Lett.* **9**, 279 (2009). Copyright © 2009 by American Chemical Society; (d) from Jeong *et al.*, *Nano Lett.* **12**, 2971 (2012). Copyright © 2012 by American Chemical Society.

by a factor of $4n^2$, where n is the refractive index of the medium. This is called the Yablonovitch limit.^{27,28} Recently, there have been studies demonstrating that nanostructures can achieve the enhancement factor beyond the Yablonovitch limit.^{29–31} The roughness of the Lambertian structure is far larger than the wavelength of light, thus the Yablonovitch limit cannot be applicable to the light trapping effect from nanostructures. In this section, we review the light trapping effect on various periodic nanostructures with a sequence of nanowires, nanoholes, nanocones, nanodomes, and nanoshells.

Ordered nanowire arrays provide the effects of scattering and collective resonances of the incident light, which can improve the light absorption. The absorption enhancement depends on several properties, such as nanowire length, diameter, and the filling ratio. In particular, the light absorption at long wavelengths are strongly dependent on the diameter of nanowires: Si nanowires with a diameter larger than a couple of hundred nanometers absorbed more light than a Si slab with a thickness equivalent to the length of the nanowires, but thinner nanowires absorbed much less light.^{32–35} Because the filling ratio was constant, this absorption difference should be explained by optical properties of nanowires. Both thinner and thicker nanowires absorbed most of short-wavelength light within less than 3 μm-long wires.^{32,33} Although the array of nanowires is geometrically porous, the light-absorbing cross section of a nanowire is bigger than its geometric cross section and the optical interactions between neighboring nanowires can suppress the transmission of short-wavelength light.³⁶ The absorption difference between thinner and thicker nanowires becomes noticeable as the wavelength becomes longer than 550 nm. Light with long wavelengths is likely to be confined in an empty space between thinner nanowires, but as the diameter of the nanowire increases, the confined field in the empty space penetrates more into the wire, increasing the absorption. Calculations showed that an array of 200–400 nm radius Si nanowires with a filling ratio of 0.3–0.6 could achieve the highest light absorption.^{32,35} Garnett *et al.* experimentally demonstrated that the optical path length was enhanced by a factor of 73 with a design of 390 nm diameter nanowires separated by 530 nm.³¹ They also studied the correlation between the roughness factor (RF) and the light trapping effect. RF was defined as the actual surface area of the structure divided by the geometric area. From the photocurrent data, they concluded that trapping efficiency clearly increased with the RF, which, they suggested, might result from photonic crystal enhancement effects of the ordered nanowire arrays (Fig. 2).

As an inverse structure of nanowires, Si nanoholes (or nanowells) were also demonstrated for the improvement of light absorption.^{37–39} The nanoholes showed similar properties of light absorption compared to nanowires: light absorption increased as the filling ratio of Si decreased or the lattice constant increased. The lower filling ratio meant less difference of refractive index between air and the Si nanostructure, which decreased reflection. Also, the larger lattice constant meant increased number of waveguide modes inside the Si nanostructures. In particular, Leung *et al.* demonstrated that

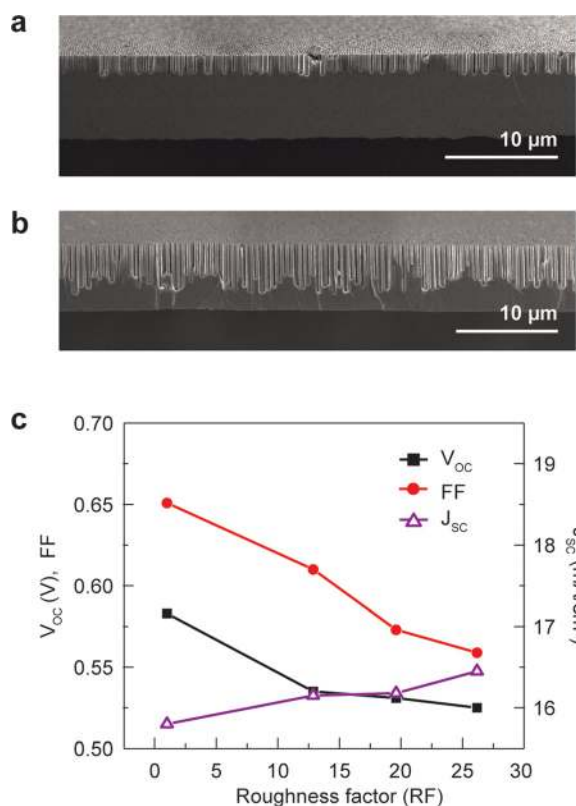


FIG. 2. (Color online) (a) and (b) Cross-sectional SEM images of (a) 2 μm long and (b) 5 μm long Si nanowires fabricated from 7.5 μm thick Si membranes. (c) The characteristics of Si nanowire array solar cells fabricated from an 8 μm thick Si layer with three different roughness factors (RF) compared to a planar structure (RF=1). Figures reproduced with permission from Garnett and Yang, *Nano Lett.* **10**, 1082 (2010). Copyright © 2010 by American Chemical Society.

the light absorption could be maximized when the diameter of nanowells was matched to the wavelength of light, as shown in Fig. 3(a).³⁹ When the diameter of nanowells was much smaller than the wavelength, most of light was reflected from the surface. In contrast, when the diameter was much larger than the wavelength, light was reflected from the bottom of the nanowells, which resulted in low absorption. The 2 μm -deep nanowells with a diameter similar to the wavelength absorbed 97.2% of the incident light. In addition, they also investigated the diffraction patterns of light (650 nm wavelength) from two arrays of nanowells: one with 1 μm diameter nanowells [Fig. 3(b)] and the other with 700 nm diameter nanowells [Fig. 3(c)]. When a grating structure diffracts the incident light to propagate along the absorber layer, the larger diffraction angle indicates the longer optical path length.^{40–44} From the simulated and measured data, the latter structure of nanowells had higher diffraction angle (73° from simulation) than the former structure (47° from simulation). The intensity of the diffraction pattern from the latter structure was much lower, thus the picture in Fig. 3(c) was taken from the sample side in much darker environment. With a proper design, the 50 nm-thick amorphous Si deposited on a template of Al nanowells achieved 94% of light absorption integrated over the wavelength range of 300–720 nm in AM 1.5 spectrum.

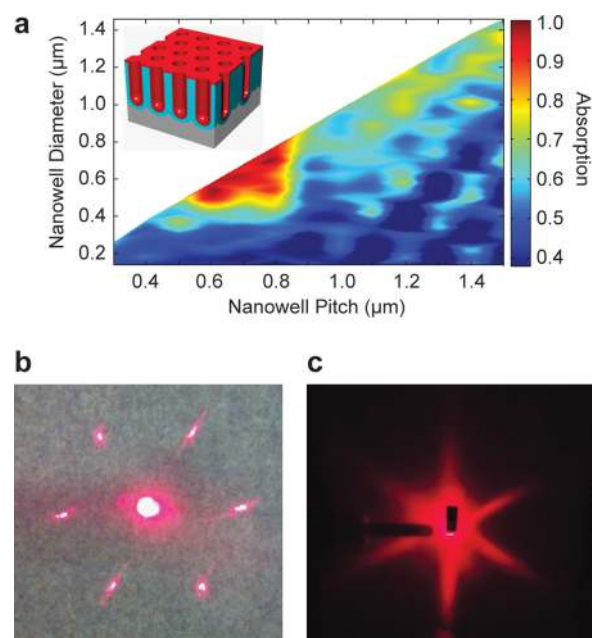


FIG. 3. (Color online) (a) Calculated absorption 2D contour of 700 nm wavelength light. Inset is a schematic of ordered nanowells with 2 μm depth. (b) and (c) Diffraction patterns of (b) 1 μm and (c) 700 nm nanowell arrays generated by 650 nm diode laser. Figures reproduced with permission from Leung *et al.*, *Nano Lett.* **12**, 3682 (2012). Copyright © 2012 by American Chemical Society.

The tapered nanostructures, such as nanocones or nanotips, can also scatter the incident light effectively into the substrate. Because the gradual change of the refractive index leads to the antireflection effect, the preferred tapered nanostructures have sharper morphology for more gradual variation, as indicated in Eq. (1). However, as the absorber thickness was decreased to tens of micrometers, it was found that the sharper nanocones were not the best choice for light absorption in a thin-film solar cell. Jeong *et al.* compared the enhancement factor of light absorption of nanocones with different aspect ratios (height/diameter of a nanocone).²² For a 500 μm thick Si substrate, higher-aspect-ratio nanocones led to higher photocurrent [Fig. 4(a)], but for a 50 μm thick one, an aspect ratio close to one resulted in the highest photocurrent [Fig. 4(b)]. When the thickness of the substrate was reduced to 10 μm , the trend became more distinct: as the aspect ratio of the nanocones was decreased from four to one, the light absorption was increased by 17% in the 10 μm thick substrate [Fig. 4(c)], which was significantly higher than 3% and -1% in the 50 μm and 500 μm case, respectively. This unexpected result can be explained by the scattering effect from the nanocones: the nanocones with an aspect ratio close to one scatter light more laterally than those with higher aspect ratios. This was confirmed by light transmission through the 50 μm thick substrates with the nanocones having different aspect ratios [Fig. 4(d)].

Ken *et al.* showed a further improvement of the light absorption with a double-sided grating design, which has nanocones on both the front and back surfaces of the substrate.⁴⁵ As shown in Fig. 5, the “double-sided” structure has an absorption spectrum very close to the Yablonovitch limit

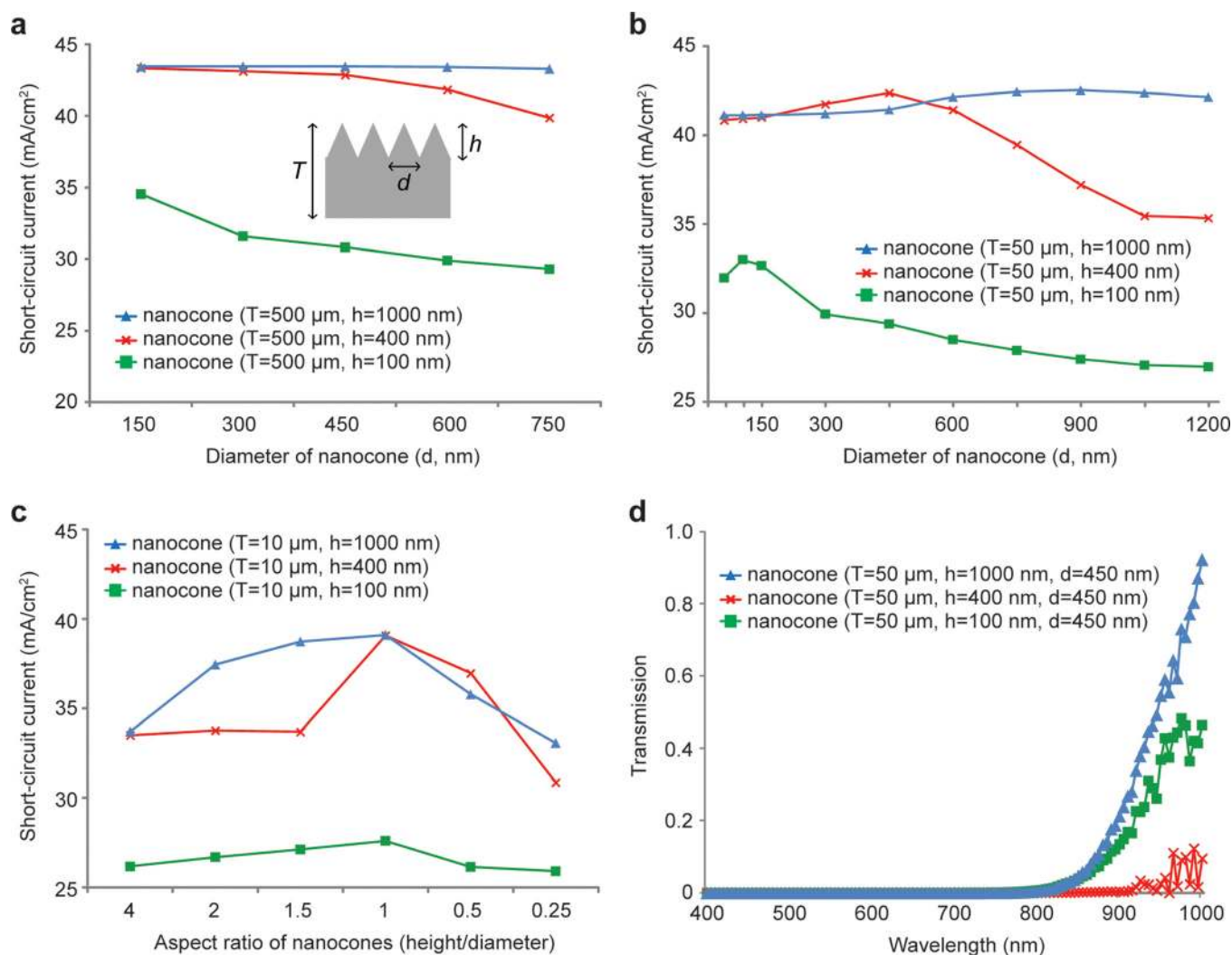


Fig. 4. (Color online) (a)–(c) Calculated J_{sc} of nanocone structures with different sizes. The total thickness of the structures is (a) $500 \mu\text{m}$, (b) $50 \mu\text{m}$, and (c) $10 \mu\text{m}$. (d) Transmission data of the three nanocone structures studied in (b). Figures reproduced with permission from Jeong *et al.*, *Nano Lett.* **12**, 2971 (2012). Copyright © 2012 by American Chemical Society.

in the wavelength range of 300–1100 nm. In the range of short wavelengths (300–800 nm), the “top-only” structure has higher absorption than the “bottom-only” structure, but in the range of long wavelengths (800–1100 nm), the former has lower absorption. Because the substrate thickness is only $2 \mu\text{m}$, the long wavelengths of light cannot be absorbed in a single path; thus, the nanocones at the back scatter the light back into the material. With the nanocones on both the front and bottom surfaces, Ken *et al.* studied the optimal periodicity of the nanocones at the bottom surface based on two considerations: a larger period leads to more guided resonances, which improves the light absorption, but each of the guided resonance modes is likely to leak to more external channels with larger period. Considering the trade-off between these two requirements, the periodicity was found to be optimal when it was close to the target wavelength of light: for Si, the optimal periodicity of the nanocones was found to be 1000 nm because light trapping is critical for the wavelength range, 800–1100 nm, near the band gap of Si. This property is similar to the study of nanowells, where the light absorption is maximized as the diameter of nanowells becomes

comparable to the wavelength.³⁹ The optimized “double-sided” Si nanocone structure is expected to yield a short-circuit current density (J_{sc}) of 34.6 mA/cm^2 with a thickness of only $2 \mu\text{m}$.

For the enhancement of light absorption in an amorphous Si (a-Si:H) solar cell, nanodome-shaped structures have been studied. Because the absorber layer in an a-Si:H solar cell was very thin (less than 400 nm), nanocone arrays were fabricated on a quartz substrate, on top of which the absorber layer, a-Si:H, was deposited. The conformal deposition of a-Si:H on top of the nanocones resulted in the nanodome shape, which can scatter light efficiently along the in-plane dimension and enhances the optical path length inside the absorber layer. This is particularly important for the long wavelength regime where a-Si:H is less absorptive. Zhu *et al.* demonstrated a nanodome-shape a-Si:H solar cell with an exceptional J_{sc} of 17.5 mA/cm^2 .⁴⁶ In addition to the nanodome structure, they used a silver (Ag) reflector with nanoscale modulation to enhance the light scattering further. Poorly absorbed light in a single path was strongly scattered by the nanoscale-modulated Ag reflector at the back, which

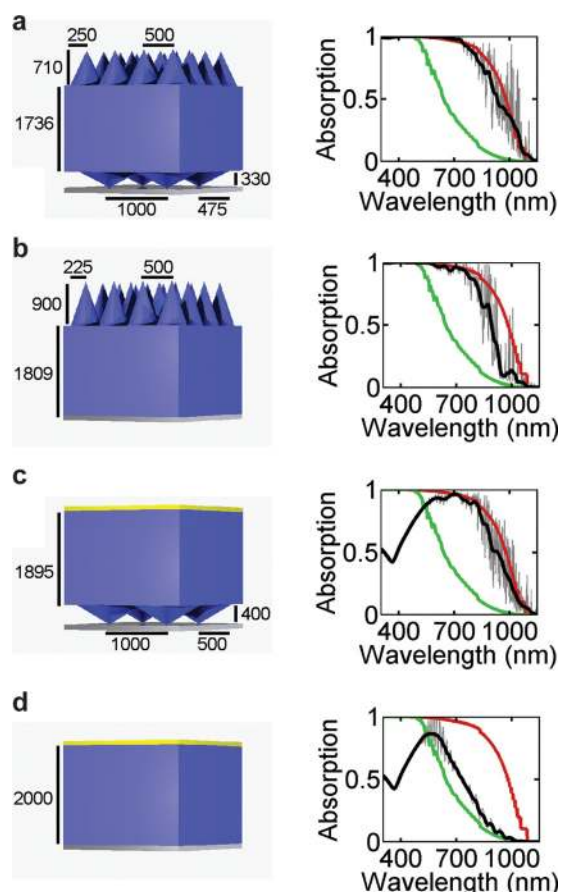


FIG. 5. (Color online) (a)–(c) Schematics and calculated optical absorption data of thin Si substrates with (a) double-sided grating, (b) top-only grating, and (c) bottom-only grating. (d) Schematic and calculated optical absorption data of a planar thin Si substrate. The unit of numbers in all the schematics is nm. The green and red lines in the absorption data represent the single-pass absorption and the Yablonoitch limit of $2\ \mu\text{m}$ thick film, and the thin and thick black lines represent the absorption data from the structures and the running averages of the absorption, respectively. Figures reproduced with permission from Wang *et al.*, *Nano Lett.* **12**, 1616 (2012). Copyright © 2012 by American Chemical Society.

resulted in the enhanced absorption. They also performed three-dimensional finite-difference time-domain (FDTD) simulations to clarify the light trapping effect on the device geometry. Figure 6 shows the simulated electric fields in the device structure for different wavelengths. Most of the light

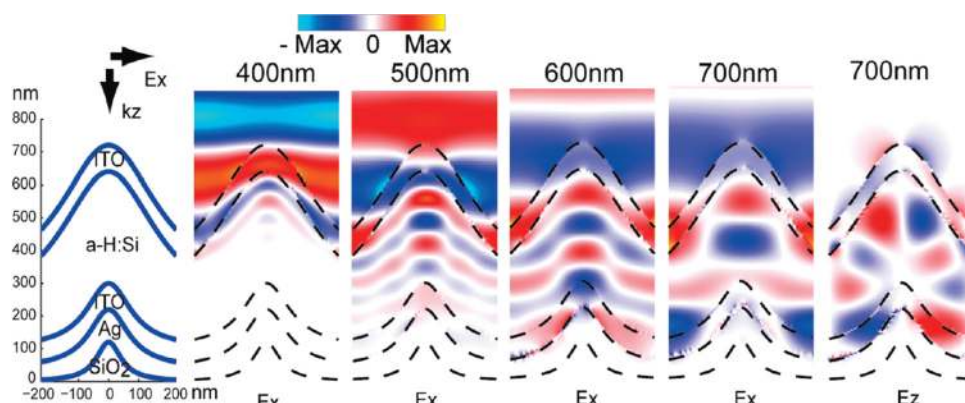


FIG. 6. (Color online) Simulated electric fields in a periodic nanodome structure of the a-Si:H solar cell for different wavelengths. Figure reproduced with permission from Zhu *et al.*, *Nano Lett.* **10**, 1979 (2010). Copyright © 2010 by American Chemical Society.

with wavelengths of 400 and 500 nm is absorbed in a single path through the a-Si:H layer. Even though the long wavelengths of light (600 and 700 nm) were not absorbed in a single path, they were strongly guided through the nanodome structure, as shown in the last panel of Fig. 6. The absorption loss due to the nanoscale modified Ag back reflector was found in a separate simulation to be only 1%, which can be neglected.

Whispering gallery mode (WGM) resonators also can be used for the light trapping in a thin-layer of Si. The WGM has been demonstrated in micrometer-sized glass spheres or toruses.^{47–49} The light is guided around the edge by the total internal reflection, leading to very high quality factor (Q), up to 10^{10} .⁴⁹ WGM resonators with high-Q values have very little energy leakage and have high-frequency selectivity at the expense of a low coupling efficiency of light into the resonator; thus, they can be used for laser cavities. In contrast, by making a low-Q WGM resonator covered with 50-nm thick Si, Yan *et al.* demonstrated up to 20-fold enhancement of light absorption.⁵⁰ The nanocrystalline Si (nc-Si) with a thickness of 50 nm was deposited conformally over a monolayer of SiO₂ nanoparticles using low-pressure chemical vapor deposition (LPCVD) method, and the particles were etched by hydrofluoric (HF) acid to make a shell structure of nc-Si, as shown in Figs. 7(a) and 9(d). The incident light was confined and guided along the shell rather than directly passing through it. The circulation (or resonance) of the light waves along the nanoshell resulted in the increase of the optical path length, thereby substantially enhancing the light absorption in such a thin layer [Fig. 7(c)]. The relatively low-Q value of the Si nanoshells not only allows efficient coupling between the incident light and resonant modes but also broadens the resonant absorption peak, which widens the absorption enhancement region.

Periodic nanostructures, such as nanowire, nanodome, nanocone, or nanoshell arrays, have been suggested in the quest to achieve higher absorption enhancement than random structures. However, the power conversion efficiencies of the solar cells fabricated on both periodic and random structures were found to be equal. Corsin *et al.* made state-of-the-art a-Si:H solar cells on top of two substrates: a periodic nanocavity formed by colloidal lithography and a random pyramid texture

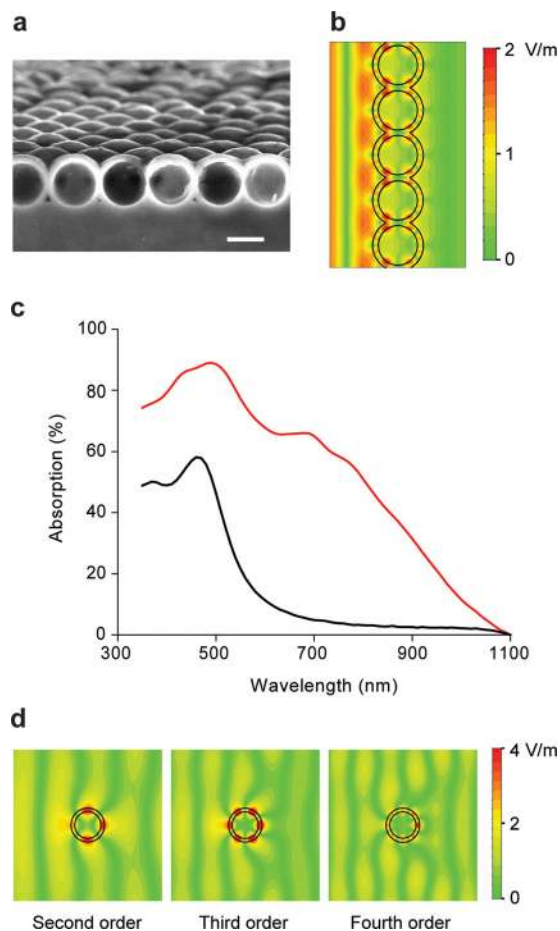


FIG. 7. (Color online) (a) Cross-sectional SEM image of a monolayer of Si spherical nanoshells. Scale bar is 300 nm. (b) Simulated electric fields in the nanoshell structure. (c) Measured optical absorption data of the nanoshells (red line) and a planar control sample (black line). (d) Electric fields coupled with a single Si nanoshell (inner radius $R_{in} = 175$ nm, outer radius $R_{out} = 225$ nm). The resonance wavelengths are 986 nm (second order), 796 nm (third order), and 685 nm (fourth order). Figures reproduced with permission from Yao *et al.*, Nat. Commun. 3, 664 (2012). Copyright © 2012 by Nature Publishing Group.

formed by low-pressure chemical vapor deposition (LPCVD), as shown in Figs. 8(a) and 8(b).⁵¹ Both cells demonstrated a significant enhancement of the external quantum efficiency (EQE) in the longer wavelength range compared to the flat morphology, but they performed differently in the range of 440–640 nm; the periodic structure showed slightly lower EQE from 440 to 540 nm than the random structure, but it performed slightly better from 540 to 640 nm [Fig. 8(c)]. Even though there are some differences in the manner in which incident light is scattered into guided modes inside material, the periodic and random structures finally showed the same power conversion efficiency.

C. Fabrication: nanostructure

Nanostructures, such as nanowires, nanocones, nanodomes, and nanoshells, have the potential to play a key role in thin-film Si solar cells. With the rapid advance of nanotechnology, various methods have been developed to make nanostructures, but in order for the nanostructures to be applicable to the pho-

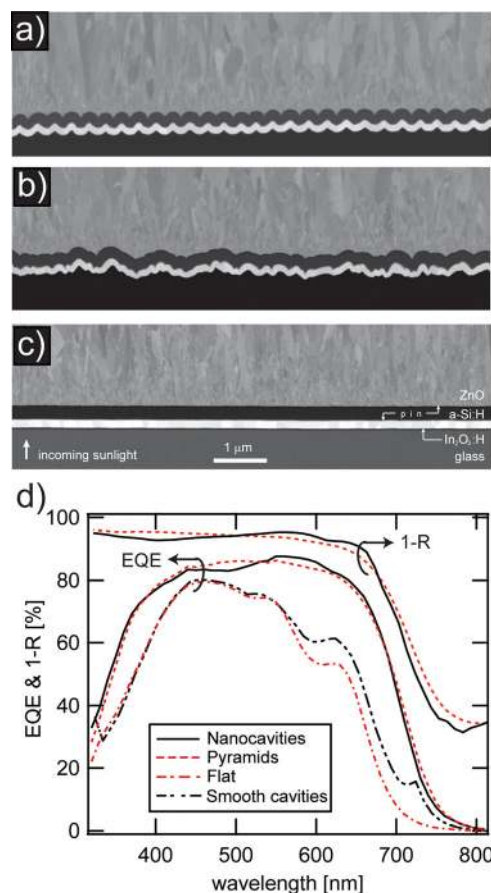


FIG. 8. (Color online) (a)–(c) Cross-sectional SEM image of the a-Si:H solar cells fabricated on (a) a periodic nanocavity structure, (b) a random pyramid structure, and (c) a planar structure. (d) The external quantum efficiency and reflectance of the three devices plotted as a function of wavelength. Figures reproduced with permission from Battaglia *et al.*, ACS Nano 6, 2790 (2012). Copyright © 2012 by American Chemical Society.

tovoltaic industry, they need to be fabricated with low-cost, high-yield, and scalable methods. One of the common methods for making nanostructures in the semiconductor industry is photolithography, which can easily make submicrometer patterns. However, this well-developed, widely used technique is expensive for making nanostructures in a solar cell. Instead, various scalable alternatives have been developed.^{52–57} Among these alternatives, colloidal lithography has been widely used because it can achieve sub-100 nm feature sizes without complex equipment.

Colloidal lithography uses two-dimensional arrays of colloidal nanospheres or microspheres as a mask: depositing metals or etching substrates through interstitial sites between these particles can easily produce nanostructures without being limited by the diffraction of light.^{58–63} One example of colloidal lithography can be explained as following: Monodispersed SiO_2 particles, with diameters from 50 to 800 nm, are synthesized by a modified Stöber process⁶⁴ and then modified with aminopropyl diethoxymethylsilane (APDEMS) in order to terminate their surface with positively charged amine groups, which prevents aggregation of the particles. These surface-functionalized particles are assembled into a close-packed monolayer on top of a substrate using the Langmuir-Blodgett (LB) method.^{65,66}

In this method, the SiO_2 particles floating on the air–water interface are pushed together horizontally to form a close-packed monolayer, and then a solid substrate is dipped vertically into the water. As the substrate is pulled up slowly, a meniscus of water at the substrate provides a capillary force, which drives the particles to form a monolayer on the substrate. The particles on the air–water interface are pushed together continuously during this process to maintain a constant input of the particles for making the monolayer. The close-packed monolayer of SiO_2 nanoparticles on a Si substrate can be used as a mask or template for the fabrication of Si nanostructures. Even though the LB method has been used in various applications, the overall processing speed is not high enough to be applicable in the photovoltaic industry. Recently, Jeong *et al.* developed a simple and scalable method: they applied a wire-wound rod coating method, which has been used in roll-to-roll processing in industry, to deposit close-packed monolayers or multilayers of SiO_2 nanoparticles on a variety of rigid and flexible substrates.⁶⁷ In this method, as the rod is pulled over the nanoparticle solution, a flat wet film is left on the substrate and the thickness of the film is determined by the size of grooves between each wire winding. As the solvent evaporates gradually from the part where it is spread first, the capillary force of the solvent gathers nanoparticles to form a monolayer. This coating technique is simple and inexpensive, and it may lead to a scalable path to implementation of nanostructures in various applications.

In order to make Si nanostructures using SiO_2 nanoparticles as a mask, the size of the particles needs to be tuned first: by reactive ion etching (RIE) with a mixture of gases, CHF_3 and O_2 , each particle can be etched to a certain size to be an etching mask for Si nanostructures. Unlike isotropic SiO_2 etching, Cl_2 based anisotropic RIE of Si can make Si nanowires and nanocones. Finally, SiO_2 nanoparticles at the tip of the nanostructures are etched with hydrofluoric (HF) acid [Figs. 9(a) and 9(b)]. Due to the well-developed Si etching technology employed in the semiconductor industry, the consistent formation of Si nanostructures over a 4-in. wafer has been demonstrated and utilized in various applications.^{18,22,68,69} A wide range of Si nanostructures can be achieved, because the diameter of Si nanostructures is determined by the size of SiO_2 particles, which can be controlled easily by synthesis methods or etching conditions. In addition, the combination of anisotropic and isotropic etching allows a sharpening of the Si tips to a radius of curvature of less than 10 nm.⁶⁸

Si nanostructures fabricated from the colloidal lithography have been demonstrated as an efficient light absorber for crystalline Si solar cells. However, for an amorphous Si solar cell (a-Si:H), which is normally fabricated by plasma enhanced chemical vapor deposition (PECVD) with a thickness of less than $1\ \mu\text{m}$, the base substrate, such as glass, must be nanostructured before the material deposition. For making nanostructures on glass, metals such as aluminum (Al) or chromium (Cr) can be a better choice for an etching mask than SiO_2 nanoparticles. At first, a monolayer of SiO_2 nanoparticles is formed on a glass substrate, and the particles are etched to a certain

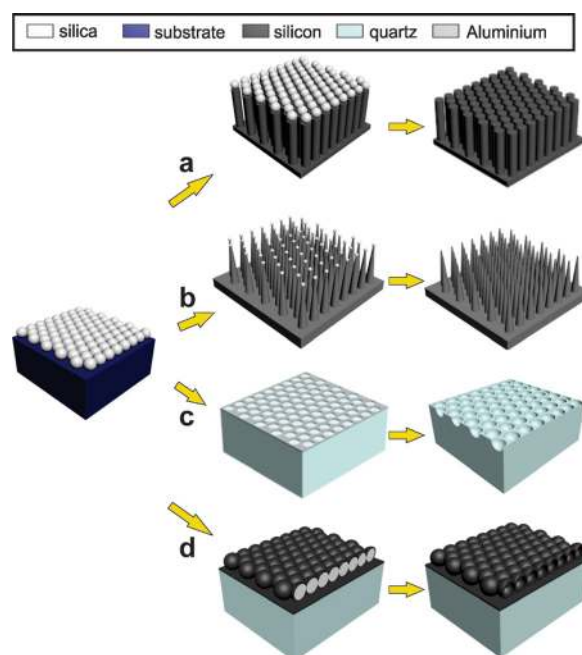


Fig. 9. (Color online) Schematics of colloidal lithography for making arrays of (a) nanowires, (b) nanocones, (c) nanowells, and (d) nanoshells.

size, as in the case of making Si nanostructures. Then, a thin layer of Al or Cr is evaporated to make a metal mesh over the glass substrate, and the particles are removed by sonication in ethanol. Finally, the reactive ion etching of the glass substrate through the metal mesh forms nanowell structures, as shown in Fig. 9(c).

The colloidal lithography method is a scalable and inexpensive alternative to make nanostructures on various materials. However, this technique includes etching steps, which can limit its applications to certain materials, such as Si or SiO_2 . In a recent report about a nonetching method for making nanocone structures, Jeong *et al.* demonstrated the formation of tin oxide (SnO_x) nanocones on various substrates, such as Si, aluminum foil, quartz, and polyimide film, by simple process steps: deposition and oxidation of a thin film of tin (Sn) in low-oxygen environments.⁷⁰ Annealing a thin-film of Sn over its melting point (232°C) in an inert gas environment with low oxygen concentration (less than 100 ppm) formed liquid-phase Sn nanoparticles. When the Sn particles became supersaturated with dissolved oxygen, the solid SnO_x started to nucleate at the interface between the liquid Sn and solid substrate. The combined factors of high surface tension of the liquid-phase Sn and the consumption of Sn as SnO_x was formed resulted in the formation of a tapered SnO_x nanocone structure [Fig. 10(a)]. They easily controlled the shape of the SnO_x nanocones, such as the aspect ratio (height divided by diameter), under different experimental conditions. Because the refractive index of SnO_x is approximately 2, which is between those of air and Si, the nanocones formed on a polycrystalline Si substrate increased the light absorption over 30% in the 400–850 nm wavelength range compared to the planar substrate, as shown in Fig. 10(c).⁷⁰ The general idea of this method is to anneal a thin film of metal above its melting temperature under low

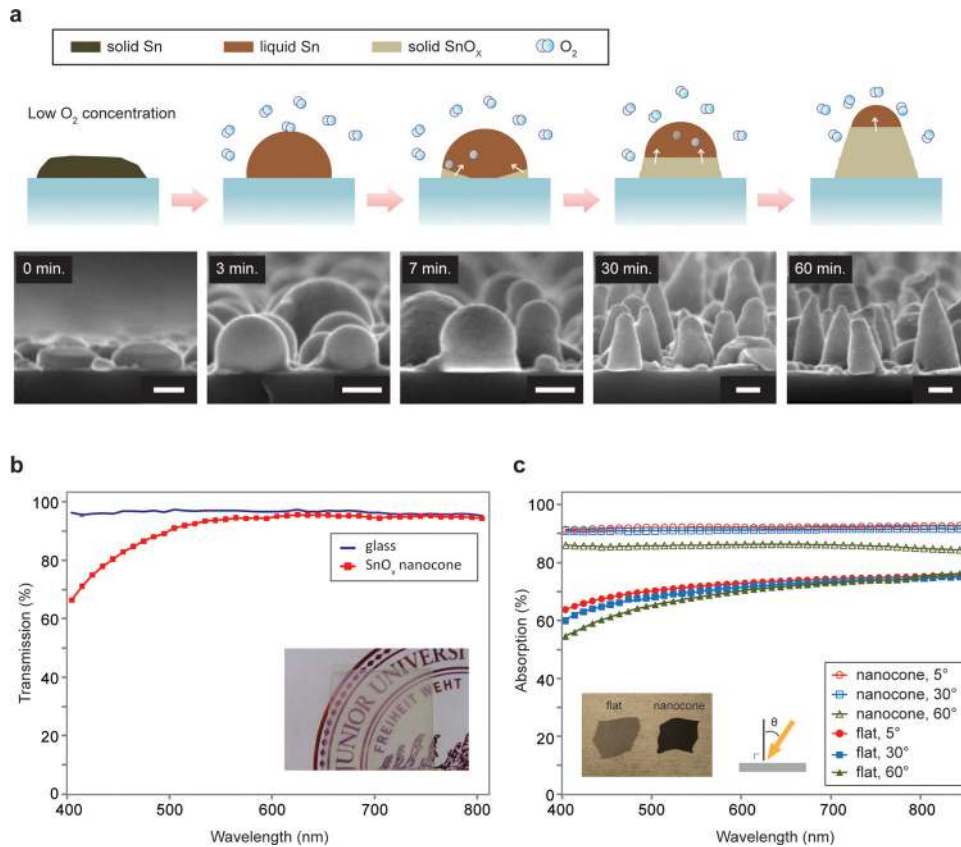


FIG. 10. (Color online) (a) Schematics and corresponding cross-sectional SEM images of the oxidation process of Sn in a nitrogen gas environment with less than 100 ppm oxygen concentration. All scale bars are 100 nm. (b) Transmission measurement data of bare glass and glass with SnO_x nanocones. (c) Absorption measurement data of polycrystalline Si substrates with and without SnO_x nanocones. All the nanocones were fabricated from 50 nm thick Sn film. Figures reproduced with permission from Jeong *et al.*, ACS Nano 5, 5800 (2011). Copyright © 2011 by American Chemical Society.

oxygen concentrations, by which method solid-phase metal oxide forms from the bottom to the top.

III. DISCUSSION

A. Challenges of nanostructure

The power conversion efficiency is the key parameter for a solar cell. Enhancement of light absorption is important, but it does not always result in efficiency improvement. Most of the photon management schemes on the nanoscale are likely to increase a saturation current density, which are attributed to the increased surface area and the defects generated during the nanoscale texturing. The increased saturation current density decreases an open-circuit voltage (V_{OC});⁷¹ thus, the enhancement of light may not improve efficiency. Garnett *et al.* demonstrated a significant enhancement of the optical path length through Si nanowire arrays, but the power conversion efficiency was less than that of the planar control device. The importance of surface passivation was explored through the comparison of the open-circuit voltage (V_{OC}) and fill factor (FF) with different roughness factors. A higher roughness factor increased the light trapping effect, which led to higher photocurrent, but it decreased the V_{OC} and FF significantly [Fig. 2(c)].

For a single-crystalline Si solar cell, most of the nanostructuring for the enhancement of light absorption has been con-

ducted by a top-down etching method. On the other hand, for an amorphous Si (a-Si:H) solar cell, whose absorber thickness is less than 300 nm, the base substrate, such as glass, is nanostructured first, and then amorphous Si is deposited on top of it. Therefore, the device performance can be dependent on the morphology of the base substrate. Hsu *et al.* fabricated amorphous Si solar cells on different nanostructured substrates, as shown in Fig. 11.⁷² Even though the final morphology of three devices fabricated on nanopillar-, nanodome-, and nanocone-shaped substrates looked similar, their current density–voltage characteristics were completely different: the former two structures led to a severe deterioration of V_{OC} and FF, but the last one maintained high V_{OC} and FF with a 20% increase in J_{SC} . The reduction in V_{OC} and FF was related to the quality of the amorphous Si layer. The amorphous Si layer deposited on top of the nanopillar substrate had deviations from conformality, which were responsible for local variations in charge carrier generation and collection. The nanodome substrate did not have the conformality issue, but it had a formation of porous, low-density material in the V-shaped valleys between the domes. This issue has already been shown to be responsible for a reduction in both V_{OC} and FF in other studies.^{73,74}

B. Another solution: plasmonic solar cells

In order to increase the light absorption while minimizing the increase in surface recombination, the plasmonic effect

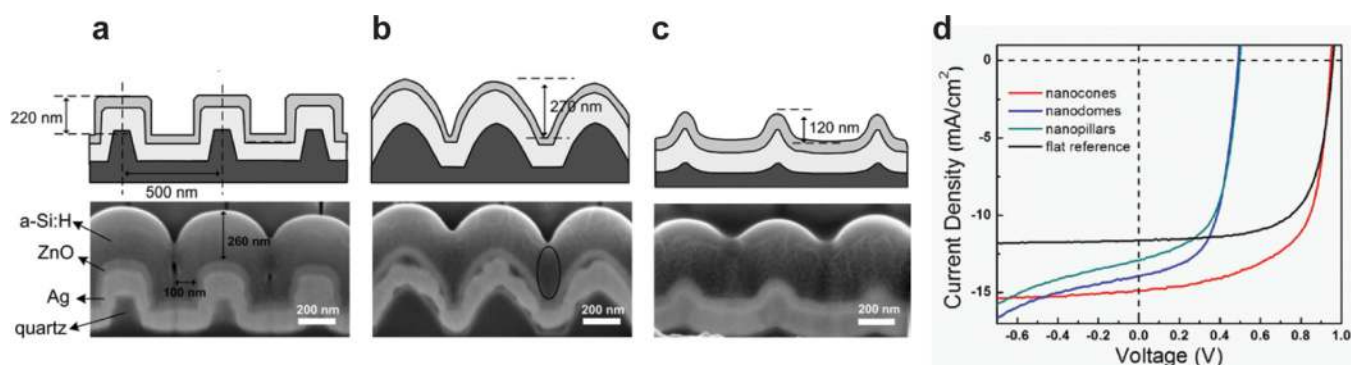


FIG. 11. (Color online) (a)–(c) Schematics and cross-sectional SEM images of a-Si:H solar cells on three different nanostructures: (a) nanopillar, (b) nanodomes, and (c) nanocone. (d) The current density—voltage (J-V) characteristics of the three devices in (a)–(c). Figures reproduced with permission from Hsu *et al.*, *Adv. Energy Mater.* **2**, 628 (2012). Copyright © 2012 by John Wiley & Sons.

has emerged as a promising method for photon management on the nanoscale. Plasmons, defined as free electron oscillations at the interface between metal and dielectric, can significantly magnify the scattering of the incident light into the guided modes of the substrate. The demonstrations of the increase in photocurrent of a thin Si layer with metal nanoparticles without the use of texturing has resulted in numerous studies to explore the plasmonic light trapping effect for very thin solar cells.^{75–84} Even though there are some disadvantages, such as unwanted charge recombinations at the metal surface and light absorption in the metal, much progress has been made with promising solutions. More details on the plasmonic solar cells can be found in other literature.^{85–89} With the development of scalable metal nanostructures and ways to minimize the disadvantages, the plasmonic effect has the potential to be widely used for a next-generation photovoltaic device.

IV. SUMMARY AND CONCLUSIONS

By 2030, the thickness of Si solar cells needs to be reduced to 80 μm for cost reduction.² In order for a thinner absorber to absorb the same amount of light as a thicker one, effective light harvesting methods must be implemented. Enhancement of light absorption can be achieved by two mechanisms: minimizing the reflection from the incident surface and increasing the optical path length inside the material. Conventional schemes for antireflection are effective within a limited spectrum of light, and their textured dimensions are not appropriate for an absorber layer with a thickness close to tens of micrometer. Nanostructures, such as nanowires or nanocones, provide a complete antireflection effect over a wide range of visible light wavelengths, and they can be implemented easily in a subwavelength thick absorber. In particular, the light absorption of the nanostructure is drastically less dependent on the incident angle than that of the planar structure, which is a critical advantage for solar cells since the incident direction of sunlight keeps changing during daytime. For light scattering inside the material, periodic nanostructures can increase the optical path length to more than the Yablonovitch limit. Light can be trapped through resonance and diffraction, which is difficult to achieve by conventional micrometer-sized textured

structures. Thus, nanostructuring for improved light absorption is a promising solution for economically viable photovoltaic devices, even though some challenges must still be addressed before the benefits can be realized commercially. Significant development of nanotechnology will accelerate the realization of photovoltaic technology as a sustainable energy solution that can support unprecedented energy needs.

ACKNOWLEDGMENTS

This work was based upon work supported as part of the Center on Nanostructuring for Efficient Energy Conversion (CNEEC) at Stanford University, an Energy Frontier Research Center funded by the U.S. Department of Energy, Office of Science, Office of Basic Energy Sciences under Award No. DE-SC0001060. S.J. acknowledges support from the Korea Foundation for Advanced Studies (KFAS) for graduate fellowship.

¹BP, BP Sustainability Review (2010).

²Advanced Research Projects Agency-Energy, U.S. Department of Energy, \$1/W Photovoltaic Systems (2010), pp. 1–28, www.bp.com/sustainability.

³P. Jackson, D. Hariskos, E. Lotter, S. Paetel, R. Wuerz, R. Menner, W. Wischmann, and M. Powalla, *Prog. Photovoltaics* **19**, 894 (2011).

⁴M. A. Green, K. Emery, Y. Hishikawa, and W. Warta, *Prog. Photovoltaics* **16**, 61 (2008).

⁵M. A. Green, K. Emery, Y. Hishikawa, W. Warta, and E. D. Dunlop, *Prog. Photovoltaics* **20**, 12 (2012).

⁶C. H. Peters *et al.*, *Adv. Mater.* **24**, 663 (2012).

⁷C. H. Peters, I. T. Sachs-Quintana, J. P. Kastrop, S. Beaupré, M. Leclerc, and M. D. McGehee, *Adv. Energy Mater.* **1**, 491 (2011).

⁸W. Shockley and H. J. Queisser, *J. Appl. Phys.* **32**, 510 (1961).

⁹C. H. Henry, *J. Appl. Phys.* **51**, 4494 (1980).

¹⁰M. A. Green, *Prog. Photovoltaics* **17**, 183 (2009).

¹¹J. Zhao, A. Wang, M. A. Green, and F. Ferrazza, *Appl. Phys. Lett.* **73**, 1991 (1998).

¹²J. Zhao, A. Wang, P. Altermatt, and M. A. Green, *Appl. Phys. Lett.* **66**, 3636 (1995).

¹³J. Zhao and M. A. Green, *IEEE Trans. Electron Devices* **38**, 1925 (1991).

¹⁴J. Q. Xi, M. F. Schubert, J. K. Kim, E. F. Schubert, M. Chen, S. Y. Lin, W. Liu, and J. A. Smart, *Nature Photon.* **1**, 176 (2007).

¹⁵S. Lien, D. Wu, W. Yeh, and J. Liu, *Sol. Energy Mater. Sol. Cells* **90**, 2710 (2006).

¹⁶S. Chhajed, M. F. Schubert, J. K. Kim, and E. F. Schubert, *Appl. Phys. Lett.* **93**, 251108 (2008).

¹⁷Y. F. Huang *et al.*, *Nature Nanotech.* **2**, 770 (2007).

¹⁸J. Zhu *et al.*, *Nano Lett.* **9**, 279 (2009).

¹⁹J. Y. Jung, Z. Guo, S. W. Jee, H. D. Um, K. T. Park, and J. H. Lee, *Opt. Express* **18**, A286 (2010).

- ²⁰Z. Fan *et al.*, *Nano Lett.* **10**, 3823 (2010).
- ²¹S. E. Han and G. Chen, *Nano Lett.* **10**, 4692 (2010).
- ²²S. Jeong, E. C. Garnett, S. Wang, Z. Yu, S. Fan, M. L. Brongersma, M. D. McGehee, and Y. Cui, *Nano Lett.* **12**, 2971 (2012).
- ²³E. D. Palik, *Handbook of Optical Constants of Solids* (Academic, San Diego, 1998).
- ²⁴J. C. Zolper, S. Narayanan, S. R. Wenham, and M. A. Green, *Appl. Phys. Lett.* **55**, 2363 (1989).
- ²⁵P. Campbell and M. A. Green, *J. Appl. Phys.* **62**, 243 (1987).
- ²⁶M. A. Green, *Prog. Photovoltaics* **10**, 235 (2002).
- ²⁷E. Yablonovitch and G. D. Cody, *IEEE Trans. Electron Devices* **29**, 300 (1982).
- ²⁸E. Yablonovitch, *J. Opt. Soc. Am.* **72**, 899 (1982).
- ²⁹Z. Yu, A. Raman, and S. Fan, *Proc. Natl. Acad. Sci. U.S.A.* **107**, 17491 (2010).
- ³⁰D. M. Callahan, J. N. Munday, and H. A. Atwater, *Nano Lett.* **12**, 214 (2012).
- ³¹E. C. Garnett and P. Yang, *Nano Lett.* **10**, 1082 (2010).
- ³²C. Lin and M. L. Povinelli, *Opt. Express* **17**, 19371 (2009).
- ³³L. Hu and G. Chen, *Nano Lett.* **7**, 3249 (2007).
- ³⁴M. D. Kelzenberg *et al.*, *Nature Mater.* **9**, 239 (2010).
- ³⁵H. Alaeian, A. C. Atre, and J. A. Dionne, *J. Opt.* **14**, 024006 (2012).
- ³⁶C. F. Bohren and D. R. Huffman, *Absorption and Scattering of Light by Small Particles* (Wiley-VCH, Weinheim, 2004).
- ³⁷S. E. Han and G. Chen, *Nano Lett.* **10**, 1012 (2010).
- ³⁸K. Q. Peng, X. Wang, L. Li, X. L. Wu, and S. T. Lee, *J. Am. Chem. Soc.* **132**, 6872 (2010).
- ³⁹S. F. Leung, M. Yu, Q. Lin, K. Kwon, K. L. Ching, L. Gu, K. Yu, and Z. Fan, *Nano Lett.* **12**, 3682 (2012).
- ⁴⁰S. H. Zaidi, J. M. Gee, and D. S. Ruby, in *28th IEEE Photovoltaic Specialists Conference* (IEEE, Anchorage, 2000), pp. 395–398.
- ⁴¹C. Heine and R. H. Morf, *Appl. Opt.* **34**, 2476 (1995).
- ⁴²M. Wellenzohn and R. Hainberger, *Opt. Express* **20**, A20 (2012).
- ⁴³S. Zanotto, M. Liscidini, and L. C. Andreani, *Opt. Express* **18**, 4260 (2010).
- ⁴⁴J. Michel and L. C. Kimerling, *IEEE Trans. Electron Devices* **54**, 1926 (2007).
- ⁴⁵K. X. Wang, Z. Yu, V. Liu, Y. Cui, and S. Fan, *Nano Lett.* **12**, 1616 (2012).
- ⁴⁶J. Zhu, C. M. Hsu, Z. Yu, S. Fan, and Y. Cui, *Nano Lett.* **10**, 1979 (2010).
- ⁴⁷C. Briggs, T. Buxkemper, L. Czaia, H. Green, and S. Gustafson, *Nature* **421**, 925 (2003).
- ⁴⁸S. L. McCall, A. F. J. Levi, R. E. Slusher, S. J. Pearton, and R. A. Logan, *Appl. Phys. Lett.* **60**, 289 (1992).
- ⁴⁹K. J. Vahala, *Nature* **424**, 839 (2003).
- ⁵⁰Y. Yao, J. Yao, V. K. Narasimhan, Z. Ruan, C. Xie, S. Fan, and Y. Cui, *Nat. Commun.* **3**, 664 (2012).
- ⁵¹C. Battaglia *et al.*, *ACS Nano* **6**, 2790 (2012).
- ⁵²K. Peng, Y. Xu, Y. Wu, Y. Yan, S. T. Lee, and J. Zhu, *Small* **1**, 1062 (2005).
- ⁵³M. Abbott and J. Cotter, *Prog. Photovoltaics* **14**, 225 (2006).
- ⁵⁴B. K. Nayak, V. V. Iyengar, and M. C. Gupta, *Prog. Photovoltaics* **19**, 631 (2011).
- ⁵⁵C. Battaglia *et al.*, *Nano Lett.* **11**, 661 (2011).
- ⁵⁶C. H. Hsu, H. C. Lo, C. F. Chen, C. T. Wu, J. S. Hwang, D. Das, J. Tsai, L. C. Chen, and K. H. Chen, *Nano Lett.* **4**, 471 (2004).
- ⁵⁷J. J. Dumond and H. Y. Low, *J. Vac. Sci. Technol. B* **30**, 010801 (2012).
- ⁵⁸H. Y. Ko, H. W. Lee, and J. Moon, *Thin Solid Films* **447–448**, 638 (2004).
- ⁵⁹S. M. Yang, S. G. Jang, D. G. Choi, S. Kim, and H. K. Yu, *Small* **2**, 458 (2006).
- ⁶⁰Y. Xia, B. Gates, Y. Yin, and Y. Lu, *Adv. Mater.* **12**, 693 (2000).
- ⁶¹P. Jiang and M. J. McFarland, *J. Am. Chem. Soc.* **127**, 3710 (2005).
- ⁶²B. G. Jung, S. H. Min, C. W. Kwon, S. H. Park, K. B. Kim, and T. S. Yoon, *J. Electrochem. Soc.* **156**, K86 (2009).
- ⁶³N. Vogel, C. K. Weiss, and K. Landfester, *Soft Matter* **8**, 4044 (2012).
- ⁶⁴G. H. Bogush, M. A. Tracy, and C. F. Zukoski IV, *J. Non-Cryst. Solids* **104**, 95 (1988).
- ⁶⁵A. Ulman, *An Introduction to Ultrathin Organic Films: From Langmuir-Blodgett to Self-Assembly* (Academic, New York, 1991).
- ⁶⁶M. Sastry, *Colloids and Colloid Assemblies*, edited by F. Caruso (Wiley-VCH, Weinheim, 2004), pp. 369–393.
- ⁶⁷S. Jeong, L. Hu, H. R. Lee, E. C. Garnett, J. W. Choi, and Y. Cui, *Nano Lett.* **10**, 2989 (2010).
- ⁶⁸C. M. Hsu, S. T. Connor, M. X. Tang, and Y. Cui, *Appl. Phys. Lett.* **93**, 133109 (2008).
- ⁶⁹E. C. Garnett, M. L. Brongersma, Y. Cui, and M. D. McGehee, *Annu. Rev. Mater. Res.* **41**, 269 (2011).
- ⁷⁰S. Jeong, M. T. McDowell, and Y. Cui, *ACS Nano* **5**, 5800 (2011).
- ⁷¹J. Nelson, *The Physics of Solar Cells* (Imperial College, London, 2003).
- ⁷²C. M. Hsu, C. Battaglia, C. Pahud, Z. Ruan, F. J. Haug, S. Fan, C. Ballif, and Y. Cui, *Adv. Energy Mater.* **2**, 628 (2012).
- ⁷³Y. Nasuno, M. Kondo, and A. Matsuda, *Jpn. J. Appl. Phys., Part 2* **40**, L303 (2001).
- ⁷⁴H. Sakai, T. Yoshida, T. Hama, and Y. Ichikawa, *Jpn. J. Appl. Phys., Part 1* **29**, 630 (1990).
- ⁷⁵H. R. Stuart and D. G. Hall, *Appl. Phys. Lett.* **73**, 3815 (1998).
- ⁷⁶D. M. Schaadt, B. Feng, and E. T. Yu, *Appl. Phys. Lett.* **86**, 063106 (2005).
- ⁷⁷S. Pillai, K. R. Catchpole, T. Trupke, and M. A. Green, *J. Appl. Phys.* **101**, 093105 (2007).
- ⁷⁸S. Mokkaṭpati, F. J. Beck, A. Polman, and K. R. Catchpole, *Appl. Phys. Lett.* **95**, 053115 (2009).
- ⁷⁹V. E. Ferry, J. N. Munday, and H. A. Atwater, *Adv. Mater.* **22**, 4794 (2010).
- ⁸⁰R. A. Pala, J. White, E. Barnard, J. Liu, and M. L. Brongersma, *Adv. Mater.* **21**, 3504 (2009).
- ⁸¹D. Derkacs, S. H. Lim, P. Matheu, W. Mar, and E. T. Yu, *Appl. Phys. Lett.* **89**, 093103 (2006).
- ⁸²V. E. Ferry, M. A. Verschuuren, H. B. T. Li, R. E. I. Schropp, H. A. Atwater, and A. Polman, *Appl. Phys. Lett.* **95**, 183503 (2009).
- ⁸³P. Matheu, S. H. Lim, D. Derkacs, C. McPheeters, and E. T. Yu, *Appl. Phys. Lett.* **93**, 113108 (2008).
- ⁸⁴J. R. Cole and N. J. Halas, *Appl. Phys. Lett.* **89**, 153120 (2006).
- ⁸⁵M. A. Green and S. Pillai, *Nature Photon.* **6**, 130 (2012).
- ⁸⁶H. A. Atwater and A. Polman, *Nature Mater.* **9**, 205 (2010).
- ⁸⁷S. B. Mallick, N. P. Sergeant, M. Agrawal, J. Y. Lee, and P. Peumans, *MRS Bull.* **36**, 453 (2011).
- ⁸⁸E. T. Yu and J. van de Lagemaat, *MRS Bull.* **36**, 424 (2011).
- ⁸⁹K. R. Catchpole, S. Mokkaṭpati, F. Beck, E. C. Wang, A. McKinley, A. Basch, and J. Lee, *MRS Bull.* **36**, 461 (2011).